RAMReS Sciences des Structures et de la Matière Vol. 9, N°2 (2025) 158 - 168
http://publication.lecames.org/index.php/mat *ISSN: 2630-1180*

Simulation and optimization of the texture of the front and rear faces of a bifacial silicon solar cell according to the base thickness

Moussa Camara[1,2], Landing Diatta[1], Moustapha Thiame[1,*], Mamoudou Touré[2], Haba Siba[2], Ousmane Fanta Camara[2]

[1]*Laboratory of Chemistry and physics of Materials, Assane Seck university, BP 523 Ziguinchor, Senegal*
[2]*Faculty of sciences, Gamal Abdel Nasser University, BP 1147 Conakry, Guinea*

Received: 06 May 2025 / Received in revised form: 04 July 2025 / Accepted: 28 November 2025

***Abstract*:**

In this study, we performed a simulation of a bifacial silicon photovoltaic (PV) solar cell using the PC1D numerical software. The dimensions of the texture on the front and rear faces of the solar cell were optimized according to the base thickness. The results clearly demonstrate the impact of the base thickness on the optimal texturing angle of the rear face. Increasing the base thickness leads to a reduction of the optimal texturing angle of the rear face. In addition, texturing of bifacial solar cells improves performance only when the base is thin. In our case, the thickness must be between 100 µm and 130 µm for the texturing of the illuminated surfaces to have a positive impact. An efficiency increase of 8.22% was achieved when the bifacial PV solar cell is textured and illuminated from the rear side.

***Keywords*:** Silicon; Bifacial solar cell; Texturing; Efficiency; Base thickness.

1. Introduction

Bifacial solar cells offer several advantages in certain application environments due to their ability to be illuminated from both sides. They perform well in vertical configurations, unlike monofacial PV cells, which are often used at fixed angles. Similarly, bifacial solar panels can be easily mounted on carports, awnings, and other coverings. Thus, they represent an ideal solution to increase efficiency with lower material costs, owing to an increase in photogenerated carriers. To optimize their parameters, bifacial solar cells are the subject of numerous simulations. In their work on modeling bifacial cells using Matlab Simulink and

* Corresponding author:
Email address: *mthiame@univ-zig.sn (M. Thiame)*
https://doi.org/10.70974/mat09225158

Mathcad, Mbodji *et al.* [1] presented a theoretical study of an n^+-p-p^+ type bifacial cell under a constant magnetic field and constant illumination. The effect of the magnetic field on photocurrent and photovoltage was described for each illumination mode.

Similarly, Sepeai *et al.* [2] studied a bifacial solar cell by optimizing the doping concentrations of the emitter, base, and back surface field (BSF) while varying the surface recombination velocities. They showed that the optimal recombination velocity at the rear surface is equal to 10^4 cm s^{-1}.

Mbao *et al.* [3] presented a theoretical study of an n^+-p-p^+ type bifacial cell under simultaneous illumination from both faces using Mathcad. They demonstrated that the minority carrier density in the base decreases with depth and becomes very low near the center of the base. They also highlighted the effect of grain size and recombination velocity at grain boundaries on minority carrier density.

Cai *et al.* [4] studied the optimal parameter ranges for silicon solar cells using the PC1D simulation software. By varying parameters such as emitter thickness, base thickness, emitter doping density, and base doping density, and analyzing the open-circuit voltage (V_{oc}) and short-circuit current (I_{sc}) from I-V curves, the optimal values of these parameters were determined. The results were validated by studying carrier transport mechanisms, including diffusion length, minority carrier lifetime, photogeneration, and conductivity. The results indicate that the best values for emitter and base thicknesses are 0.1 µm and 100 µm, respectively.

Furthermore, several studies have shown that solar cell efficiency improves when the illuminated face is textured, as texturing increases the absorption of incident photons [5–9]. Fang *et al.* [7] analyzed the influence of pyramid texture uniformity on defects to improve the photoelectric conversion efficiency of monocrystalline silicon solar cells. The pyramid texture uniformity was quantitatively characterized by a uniformity coefficient for each group of wafers. By adjusting this coefficient, they obtained the texturing process parameters corresponding to the maximum uniformity, enabling effective optimization to improve cell efficiency.

To overcome the low light absorption of incident photons in crystalline silicon (c-Si) solar cells due to their indirect band gap and low absorption coefficient, Abdulkadir *et al.* [8] investigated the influence of texture size on enhancing broadband light absorption in microtextured/nanotextured hybrid c-Si for solar cell applications. Microscopic pyramids were etched onto c-Si using a sodium hydroxide solution. After 30 minutes of etching, a series of pyramids with heights ranging from 3 to 7 µm and widths from 3 to 10 µm were formed. The results, after nanowire formation, show a 14.1% increase in the maximum short-circuit current density compared to pyramids without nanowires.

Also, to reduce the reflection loss of crystalline silicon solar cells, Xu *et al.* [9] proposed an optical functional film with a pyramidal texture. The results indicate that the reflection loss of smooth surface crystalline silicon cells decreased from 22.3% to 7.2% by using the triangular pyramid textured film. In the same vein, Hirpara *et al.* [10] studied the optimization of texturing parameters on a bifacial solar cell using machine learning. The results highlight the importance of surface texture in modulating front- and rear-side reflectance, which in turn influences overall solar cell performance. Pyramid structures with a base angle of 62° and a height of 3 µm can reduce reflectance by 9% while maximizing solar cell efficiency to 23.61%.

In our study, a detailed description and simulation of an n^+-p-p^+ type textured bifacial PV cell was carried out using PC1D. This structure was chosen because of the excellent results obtained from it. In an experimental study, Cuevas *et al.* [11] found that the front surface recombination velocity is equal to 2×10^5 cm s^{-1} and 3×10^6 cm s^{-1} for a bare passivated solar cell and a metallized passivated solar cell, respectively.

In this work, we optimize the texturing

parameters on the front and rear faces of a bifacial solar cell as a function of base thickness. Furthermore, the optimal electrical parameters for illumination from the front or rear faces are determined.

2. Materials and methods

Numerical simulation plays an essential role in the design, development, and performance analysis of solar cells. It significantly reduces time and costs by optimizing process steps and material choices. In this study, we optimize bifacial solar cells of the n^+-p-p^+ type using PC1D software. Figure 1 shows the configuration of the textured bifacial solar cell.

As shown in Figure 1, the process parameters studied are emitter thickness, texturing depth, texturing angle, and base thickness. Studying these parameters leads to a better understanding of their impact on performance. The optimized parameters can then serve as a starting point for the solar cell manufacturing process. Table 1 summarizes the fixed parameters in our baseline model. During the simulation, all other parameters were set to their default values except for the specifically declared ones.

3. Results and discussion

In this section, we determine some optimal parameters of the bifacial PV solar cell and provide a deeper understanding of how these parameters affect its performance.

3.1. Determination of the optimal emitter thickness

To optimize the emitter thickness, Figure 2 shows the efficiency profile as a function of emitter thickness for different base thickness values, for a bare passivated bifacial cell (a) and a metallized passivated bifacial cell (b).

According to previous studies, the emitter thickness represents only 0.6% to 10% of the total solar cell thickness [12]. To probe its influence, we varied the emitter thickness from 0.2 µm to 2 µm while keeping other parameters fixed.

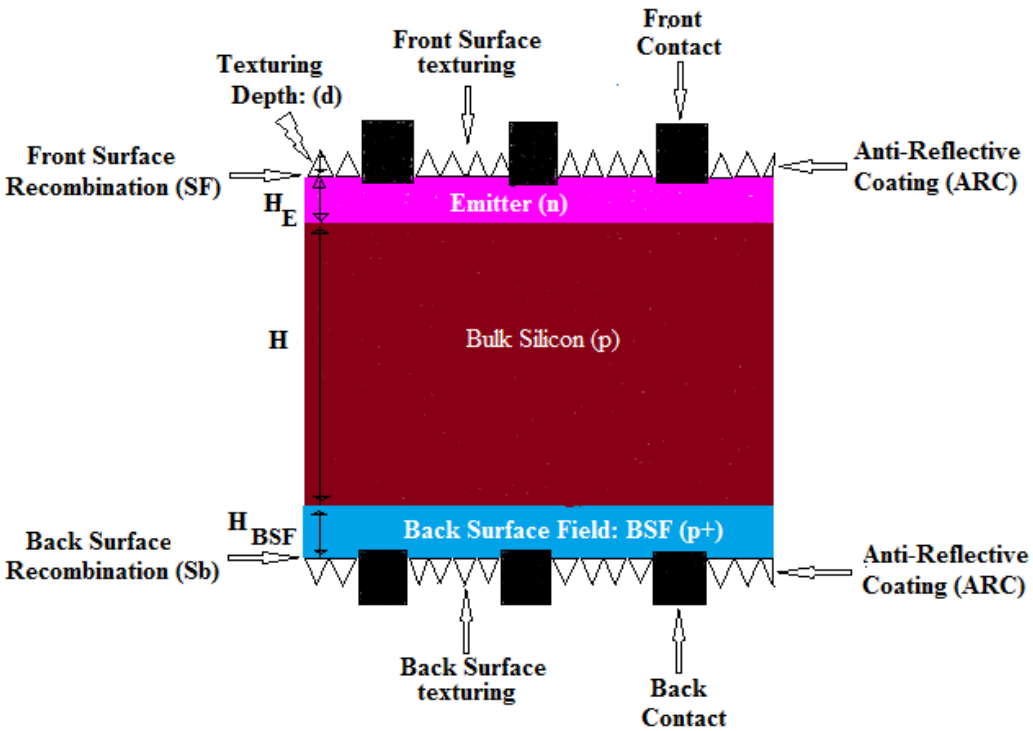

Fig. 1. Configuration of a textured bifacial PV solar cell.

Table 1
Parameters set for the simulation.

Parameter	Value
Device area	100 cm^2 [2]
Front surface texture depth	-
Rear surface texture depth	-
Front / Rear surface coating	SiN, 70 nm
Internal / external optical reflectance	10%
Base contact	-
Internal conductor	-
Thickness	-
Material	Silicon
Carrier mobilities (μ_e / μ_h)	1450 cm^2 V^{-1} s^{-1}; 413 cm^2 V^{-1} s^{-1} [2]
Dielectric constant	11.9
Band gap	1.124 eV
Intrinsic concentration at 300 K	10^{10} cm^{-3}
Absorption coefficient	Silicon
Free carrier absorption enabled	Yes
P-type background doping	10^{16} cm^{-3} [4]
Front diffusion: n-type	10^{20} cm^{-3} [2]
Rear diffusion: p-type	10^{20} cm^{-3} [2]
Bulk recombination lifetime	1000 µs
Front surface recombination velocity	10^5 cm s^{-1} / 10^6 cm s^{-1} [11]
Rear surface recombination velocity	10^4 cm s^{-1} [2]
Temperature	300 K
Bias voltage	-0.8 to 0.8 V
Light source	Front / Rear
Constant intensity	0.1 W cm^{-2}
Spectrum	AM 1.5G

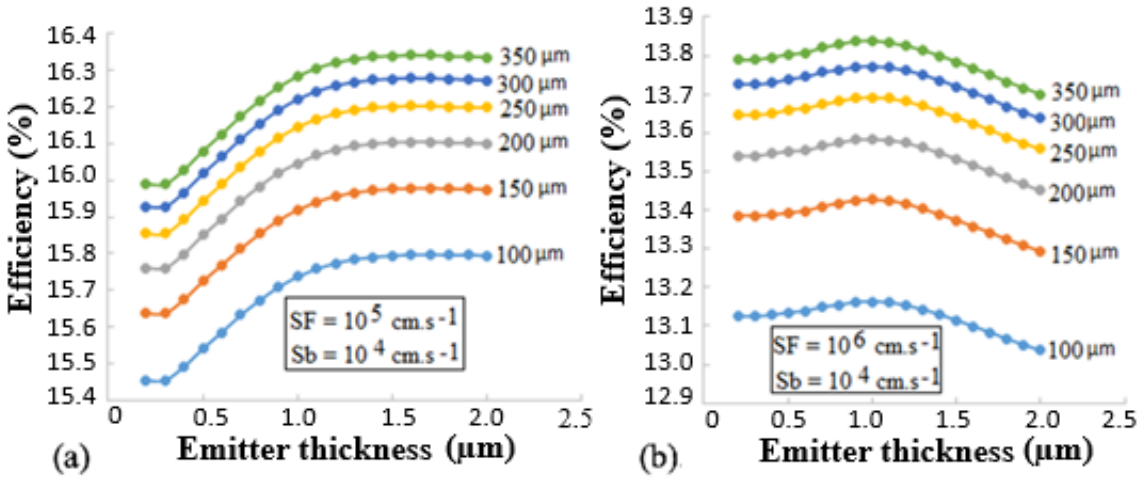

Fig. 2. Conversion efficiency as a function of emitter thickness for different base thickness values.

The results in Figure 2 reveal that efficiency increases slightly when the emitter thickness is less than 1.5 µm for the bare passivated cell and 1 µm for the metallized passivated cell. Beyond these values, efficiency decreases as emitter thickness increases.

Typically, the emitter region is doped 2 to 3 orders of magnitude higher than the base, resulting in high recombination and short diffusion lengths. The diffusion length, defined as the average distance carriers travel before recombining [13], is an important parameter for performance. The short diffusion length in the emitter is attributed to high dopant densities. The collection probability is a function of device dimensions and diffusion length [14]. If the emitter thickness is one or more orders of magnitude smaller than the diffusion length, the collection probability increases significantly [15, 16]. A higher collection probability means more photogenerated carriers are collected by the p-n junction and conducted out of the cell, thus increasing efficiency. In our study, the optimal emitter thickness is 1.5 µm for bare passivated cells and 1 µm for metallized passivated cells. Beyond these values, increasing emitter thickness degrades conversion efficiency due to increased minority carrier recombination. Figure 2 also shows that base thickness has no effect on the optimal emitter thickness.

3.2. Determination of the optimal front face texturing depth

To study the effect of front face texturing depth, Figure 3 plots efficiency as a function of texturing depth when the front surface recombination velocity (S_F) is 10^5 cm s^{-1} for a bare passivated cell (a) and 10^6 cm s^{-1} for a metallized passivated cell (b).

Figure 3 shows that efficiency increases slightly for texturing depths (d) from 0.5 µm to 2 µm. Beyond this range, efficiency decreases with increasing texturing depth. This is for a fixed texturing angle of 54.74°, an emitter thickness of 1 µm, and a base thickness of 150 µm. The curves also reveal that texturing depth has a greater impact on the efficiency of the metallized passivated cell than on the bare passivated cell.

3.3. Optimization of the front face texturing angle

To evaluate the effect of the front face texturing angle, Figure 4 shows the conversion efficiency profiles as a function of the texturing angle. The emitter thickness, base thickness, and texturing depth were fixed at 1 µm, 150 µm, and 2 µm, respectively.

Figure 4 shows an increase in efficiency for texturing angles between 10° and 70° for the bare passivated cell (a) and between 10° and 60° for the metallized passivated cell (b). Beyond these intervals, efficiency decreases with increasing texturing angle.

Silicon texturing is used to reduce surface reflectivity. This process creates a micrometric relief, typically pyramidal, on the surface.

The principle of multiple reflections reduces front surface reflection. For example, a ray at normal incidence on a pyramid can be reflected onto an adjacent pyramid, reducing the total reflection coefficient. This increases the optical path length within the silicon, enhancing photon absorption [17] and consequently cell efficiency. Surface texturing leads to greater light trapping. For angles greater than 70° (bare) or 60° (metallized), the efficiency reduction is explained by a decrease in the amount of trapped light.

3.4. Determination of the optimal rear face texturing angle

This part focuses on optimizing the rear face texturing angle for different base thicknesses. Figure 5 shows the efficiency profile as a function of the rear face texturing angle for low base thicknesses (100 µm to 130 µm) and high base thicknesses (140 µm to 190 µm), in steps of 10 µm, for both bare and metallized cells. The optimal front texturing depth of 2 µm is used for the rear face, and the emitter thickness is fixed at 1 µm.

Figure 5 shows that efficiency improves with increasing texturing angle up to an optimal angle (θ_{opt}). Beyond θ_{opt}, a strong reduction in efficiency occurs for all base thicknesses. The optimal texturing angle decreases slightly as base thickness increases in the low thickness range. It is equal to 50° for base thicknesses between 140 µm and 190 µm. Thin base thicknesses are more sensitive to rear face texturing.

For low thicknesses (100 µm to 130 µm),

efficiency values for different texturing angles are given in Tables 2 and 3 for the bare and metallized cells, respectively.

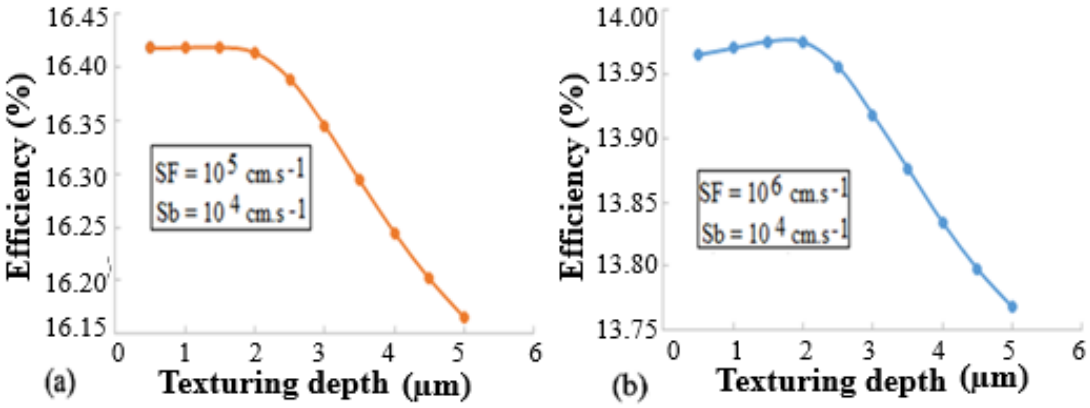

Fig. 3. Conversion efficiency as a function of front face texturing depth (d).

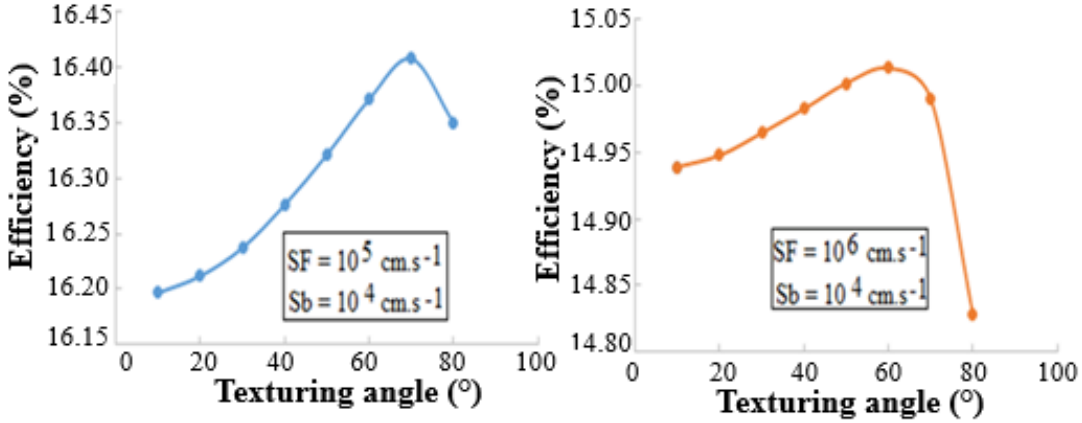

Fig. 4. Conversion efficiency as a function of front face texturing angle.

Table 2
Efficiency (%) versus texturing angle for low base thicknesses of the bare solar cell.

Texturing angle (°)	Base thicknesses (μm)			
	100	110	120	130
10	14.5435	14.623	14.688	14.7436
20	14.5614	14.6388	14.7027	14.7556
30	14.5912	14.6648	14.7252	14.7747
40	14.6317	14.6994	14.7543	14.7984
50	14.6790	14.7378	14.7841	14.8400
60	14.7201	14.7646	**14.7972**	**14.8199**
65	**14.7236**	**14.7681**	14.7937	14.8165
70	14.7065	14.7254	14.7333	14.7322
80	14.3757	14.3329	14.2809	14.2189

On the rear face, there exists a critical angle of incidence beyond which part of the light ray undergoes multiple reflections on the texture, extending its path within the semiconductor and thereby increasing photon absorption. This explains the increase in efficiency with the rear face texturing angle.

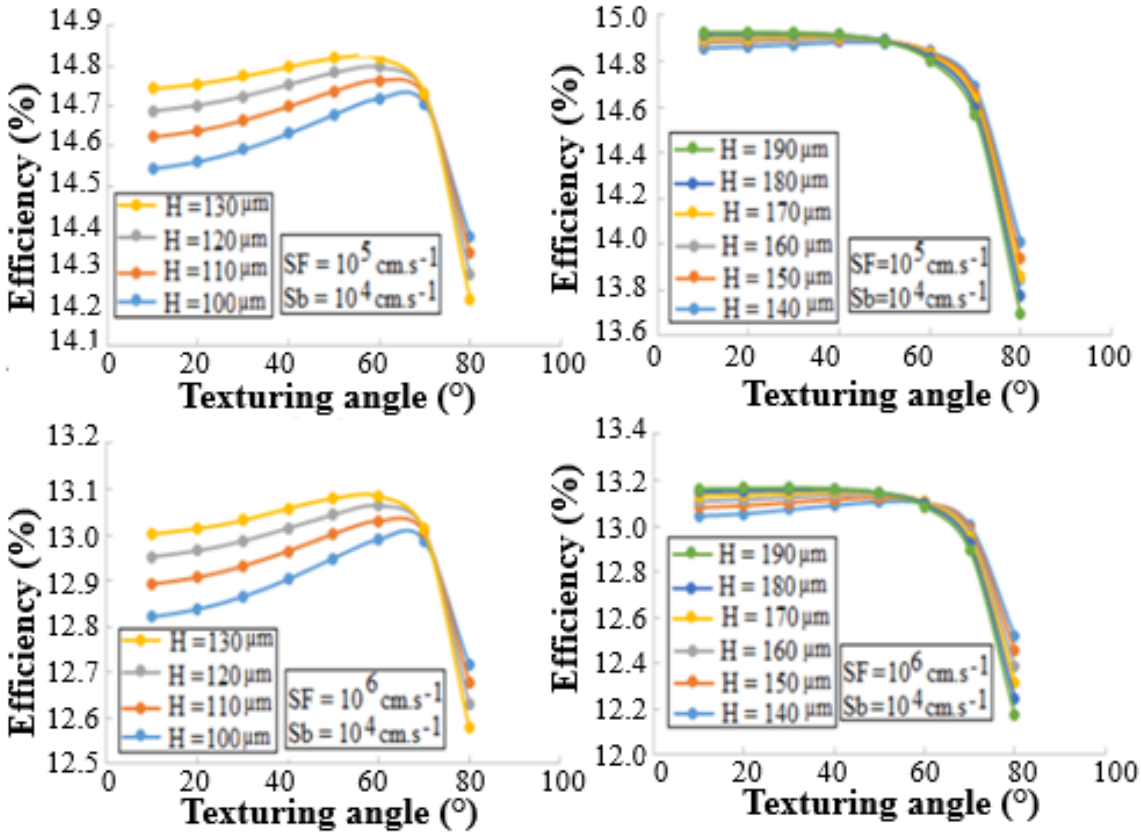

Fig. 5. Conversion efficiency as a function of rear face texturing angle for different base thicknesses (texturing depth fixed at 2 µm).

Table 3
Efficiency values depending on the texturing angle for small thicknesses of the metallized solar cell.

Texturing angle (°)	Base thicknesses (μm)			
	100	110	120	130
10	12.8208	12.8927	12.9525	13.0022
20	12.8375	12.9075	12.9656	13.0137
30	12.8652	12.9319	13.9868	13.0319
40	12.9033	12.9648	13.0147	13.0579
50	12.9487	13.0021	13.0443	13.0801
60	12.9905	13.0311	**13.0638**	**13.0848**
65	**12.9955**	**13.0367**	13.0603	13.0809
70	12.9878	13.0052	13.0127	13.0119
80	12.7164	12.6779	12.6312	12.5778

The effect of the rear face texturing angle on efficiency is significant for thin solar cells. This allowed us to optimize the base thickness. We considered two base thickness intervals: 100 µm to 130 µm (thin) and 140 µm to 190 µm (thick) (Figure 5). In both cases, efficiency increases with base thickness when the texturing angle is below θ_{opt}. Conversely, an inversion of the base thickness effect is observed when the texturing angle exceeds θ_{opt}. Increasing base thickness allows absorption of more photons, exciting more electrons and thus increasing efficiency [4].

When the base thickness varies from 100 µm to 130 µm, the rear face texturing angle has a greater impact on efficiency, while its impact diminishes from 140 µm to 190 µm, where texturing has almost a negligible effect on efficiency for both cell types. Thus, the optimal base thickness is 130 µm for both types of bifacial solar cells. We conclude that texturing the faces of a bifacial cell is more beneficial when the base is thin.

Tables 4 and 5 present the optimal texturing depth and angle for front illumination, and the optimal rear texturing angle for different base thicknesses under rear illumination, respectively.

3.5. Determination of electrical parameters of the bifacial PV solar cell

From the I-V and P-V curves, we extracted key electrical parameters: short-circuit current I_{sc} (A), open-circuit voltage V_{oc} (V), maximum power P_m (W), fill factor FF (%), and conversion efficiency η (%). Table 6 lists these values for bare and metallized passivated bifacial PV cells with optimal parameters. Table 7 compares our results with literature.

A comparative study of electrical parameters for non-textured and textured bifacial silicon solar cells (with our optimal parameters) is presented in Table 8, for a metallized cell illuminated from the rear side.

A clear improvement in electrical parameters is observed when the solar cell is textured on the rear face, with an 8.22% increase in produced power. Considering both illuminated sides, our results are consistent with those of Hirpara *et al.* [10], who obtained a 9% absorption improvement with a maximum efficiency of 23.61%.

Table 4
Optimal parameters for front-face illumination.

Parameter	Bare passivated	Metallized passivated
Optimal emitter thickness (µm)	1.5	1
Optimal base thickness (µm)	130	130
Optimal texturing depth, d_{opt} (µm)	2	2
Optimal front texturing angle, $\theta_{opt,front}$ (°)	70	60

Table 5
Optimal rear face texturing angles.

Base thickness	100 µm to 110 µm	120 µm to 130 µm	140 µm to 190 µm
$\theta_{opt,rear}$ (°)	65°	60°	50°

Table 6
Electrical parameters of the two bifacial solar cell types with optimal parameters.

	Front illumination		Rear illumination	
Parameter	Bare passivated	Metallized passivated	Bare passivated	Metallized passivated
I_{sc} (A)	0.3377	0.3275	0.3229	0.3229
V_{oc} (V)	0.5965	0.5404	0.5908	0.5420
P_m (W)	0.1644	0.1436	0.1590	0.1421
FF (%)	81.61	81.14	83.347	81.19
η (%)	16.44	14.36	15.90	14.21

Table 7
Comparison of optimal parameters with literature.

	Front illumination		Rear illumination	
Parameter	Simulation	Literature	Simulation	Literature
S_F (cm s^{-1})	10^5	10^5 [11]	10^5	10^5 [11]
H_{opt} (µm)	130	200 [1], 140 [4]	130	200 [1]
d_{opt} (µm)	2	2.5 [4]	2	-
$P_{m,opt}$ (W)	0.1644	0.1642 [2]	0.1590	0.1418 [2]
η_{opt} (%)	16.44	16.42 [2]	15.90	14.18 [2]

Table 8
Comparison of textured and non-textured bifacial solar cells (metallized, rear illumination) using optimal parameters.

Parameter	Textured	Non-textured
I_{sc} (A)	0.3229	0.3210
V_{oc} (V)	0.5420	0.5421
FF (%)	81.19	75.45
P_m (W)	0.1421	0.1313
η (%)	14.21	13.13

4. Conclusion

In this work, process parameters influencing the performance of textured front and rear face bifacial silicon solar cells were investigated for bare passivated and metallized passivated cells.

The best emitter thicknesses were found to be 1.5 µm and 1 µm for bare and metallized passivated cells, respectively. The optimal front face texturing angle is 70° for bare cells and 60° for metallized cells. The optimal rear face texturing angle is 65° for base thicknesses from 100 µm to 110 µm, 60° for thicknesses from 120 µm to 130 µm, and 50° for thicknesses from 140 µm to 190 µm.

The optimal wafer thickness for bifacial solar cells was determined to be between 100 µm and 130 µm. The results show an 8.22% increase in conversion efficiency after texturing when the solar cell is illuminated from the rear side.

References

[1] S. Mbodji, A. Diallo Ly, I. Ly, F.I. Barro, F. Zougmore, G. Sissoko, *Equivalent electric circuit MATLAB Simulink of a Bifacial Solar Cell in Transient State, Applied Magnetic Field Effect*, J. Sci. 6 (2006) 99-104.

[2] S. Sepeai, S.H. Zaidi, M.K.M. Desa, M.Y. Sulaiman, N.A. Ludin, M. Adib Ibrahim, *Design Optimization of Bifacial Solar Cell by PC1D Simulation*, Solar Energy Research Institute (SERI), Universiti Kebangsaan Malaysia (UKM) 3(5) (2013) 2225-0573. https://doi.org/10.15377/2410-2199.2013.01.01.1

[3] O. Mbao, M. Thiame, I. Ly, I. Datta, M.S. Douf, Y. Traoré, M. Ndiaye, G. Sissoko, *3D Study of a Polycrystalline Bifacial Silicon Solar Cell, Illuminated Simultaneously by Both Sides: Grain Size and Recombination Velocity Influence*, IJSET-International Journal of Innovative Science, Engineering and Technology 3(12) (2016) 2348-7968.

[4] X. Cai, X. Zhou, Z. Liu, F. Jiang, Q. Yu, *An in-depth analysis of the silicon solar cell key parameters' optimal magnitudes using PC1D simulations*, Optik 158 (2018) 105-113. https://doi.org/10.1016/j.ijleo.2017.12.069

[5] C. Ternon, A. Kaminski, D. Constantin, L. Claudon, F. Volpi, L. Vincent, Q. Rafhay, A. Bsiesy, *Simulation, élaboration et caractérisation de cellules photovoltaïques*, J3eA, Journal sur l'enseignement des sciences et technologies de l'information et des systèmes 14 (2015) 1-11. https://doi.org/10.1051/j3ea/2015001

[6] O. Gunawan, K. Wang, B. Fallahazad, Y. Zhang, E. Tutuc, S. Guha, *High Performance Wire Array Silicon Solar Cells*, Prog. Photovolt: Res. Appl. 19 (2011) 307-312. https://doi.org/10.1002/pip.1036

[7] Z. Fang, Z. Xu, D. Wang, H. Li, *The influence of the pyramidal texture uniformity and process optimization on monocrystalline silicon solar cells*, Journal of Materials Science: Materials in Electronics 31 (2020) 6295–6303. https://doi.org/10.1007/s10854-020-03186-0

[8] A. Abdulkadir, M. Almohaimeed, A.K. Isiyaku, R. Abdalrheemd, M. Isah, M.M. Aliyu, A.Y. Tanko, *Influence of micro-texture sizes towards light absorption improvement in hybrid microtextured/nanotextured black silicon for solar cells*, International Journal of Nanoelectronics and Materials 17(3) (2024) 428-436. https://doi.org/10.58915/ijneam.v17i3.359

[9] Z. Xu, X. Xu, C. Cui, *Optical functional film with triangular pyramidal texture for Crystalline silicon solar cells*, Solar Energy 201 (2020) 45-54. https://doi.org/10.1016/j.solener.2020.02.074

[10] D. Hirpara, P. Zala, M. Bhaisare, C.M. Kumar, M. Gupta, M. Kumar, B. Tripathi, *Exploring optimal pyramid textures using machine learning for high-performance solar cell production*, Journal of Computational Electronics 24 (2025) 14. https://doi.org/10.1007/s10825-024-02206-0

[11] A. Cuevas, P.A. Basore, G. Giroult-Matlakowski, C. Dubois, *Surface recombination velocity of highly doped n-type silicon*, J. Appl. Phys. 80 (1996) 3370-3375. https://doi.org/10.1063/1.363211

[12] A.B. Nawale, R.A. Kalal, A.R. Chavan, T.D. Dongale, R.K. Kamat, *Numerical investigation of spatial effects on the silicon solar cell*, J. Nano-Electron. Phys. 8 (2016) 020021-020024. https://doi.org/10.21272/jnep.8(2).02021

[13] Z.Z. Bandic, P.M. Bridger, E.C. Piquette, T.C. McGill, *Electron diffusion length and lifetime in p-type GaN*, Appl. Phys. Lett. 73 (1998) 3276-3278. https://doi.org/10.1063/1.122743

[14] S. Bowden, Collection Probability, PVEducation, (2018). https://www.pveducation.org/pvcdrom/collection-probability

[15] S.Y. Lien, D.S. Wuu, *Simulation and Fabrication of Heterojunction Silicon Solar Cells from Numerical Computer and Hot-Wire CVD*, Prog. Photovolt: Res. Appl. 17 (2009) 489-501. https://doi.org/10.1002/pip.889

[16] A. Cuevas, Characterisation and Diagnosis of Silicon Wafers and Devices, In "T. Markvart (Ed.), Solar Cells: Materials, Manufacture and Operation", Elsevier Ltd., UK (2005) 164-214. https://doi.org/10.1016/B978-18561 7457-2/50010-4

[17] O. Nichiporuk, Simulation, Fabrication et Analyse de Cellules Photovoltaïques à Contacts Arrières interdigités, Ph.D. Thesis, Institut National des Sciences Appliquées de Lyon (2005) 28.